arXiv:1402.3968v1 [nucl-th] 17 Feb 2014

Antineutron and antiproton nuclear interactions at very low energies

E. Friedman[a]

[a]*Racah Institute of Physics, The Hebrew University, 91904 Jerusalem, Israel*

Abstract

Experimental annihilation cross sections of antineutrons and antiprotons at very low energies are compared. Features of Coulomb focusing are observed for $\bar{p}$ annihilation on protons. Direct comparisons for heavier targets are not straightforward due to lack of overlap between targets and energies of experimental results for $\bar{p}$ and $\bar{n}$. Nevertheless, the annihilation cross sections for $\bar{n}$ on nuclei cannot be described by an optical potential that fits well all the available data on $\bar{p}$ interactions with nuclei. Comparisons made with the help of this potential reveal in the $\bar{n}$ data features similar to Coulomb focusing. Direct comparisons between $\bar{n}$ and $\bar{p}$ annihilations at very low energies would be possible when $\bar{p}$ cross sections are measured on the same targets and at the same energies as the available cross sections for $\bar{n}$. Such measurements may be possible in the foreseeable future.

Keywords: antineutron-nucleus and antiproton nucleus interactions.

1. Introduction

Experimental results for annihilation cross sections of antineutrons on several nuclei at very low momenta across the periodic table have been published by the OBELIX collaboration more than a decade ago [1]. Exceedingly large cross sections have been reported below 180 MeV/c and features typical of reactions taking place at the nuclear surface have been noted. However, quantitative analyses of those data in terms of optical potentials have not been reported. In contrast, data for antiproton-nucleus interaction both below threshold (antiprotonic atoms) and above have been repeatedly analysed

*elifried@cc.huji.ac.il

and led to fully consistent quantitative picture of the interaction at low energies [2].

Comparing between $\bar{p}$ and $\bar{n}$ interactions with nuclei, it is unfortunate that experimental results are available mostly for different nuclei at different energies so that direct comparisons are not possible. Only for $\bar{p}$ and $\bar{n}$ interaction with the proton is it possible to compare directly experimental results. For nuclei we adopt an optical model as a tool for comparisons between different results. Optical potentials simply related to nuclear densities have a long history in nuclear physics of smoothly interpolating values of observables over energy and over atomic and mass numbers [3]. It is shown in the present work that such an approach which is successful for $\bar{p}$-nucleus interactions poses problems when applied to antineutrons.

In sec.2 we compare total annihilation cross sections for $\bar{p}p$ and $\bar{n}p$ at very low energies and describe the mechanism of Coulomb focusing which is responsible for large differences at low energies. In sec.3 we re-examine results for antiproton-nucleus interactions at low energies showing the high degree of consistency between the various experimental results along the periodic table, both below and above threshold. In sec.4 we confront the experimental annihilation cross sections for $\bar{n}$ on nuclei with various calculations. The increased importance at low energies of Coulomb focusing is discussed in some detail.

Section 5 is a discussion where it is proposed to match the existing data of annihilation cross sections for $\bar{n}$ on nuclei by measuring annihilation cross sections for $\bar{p}$ on the same nuclei at the corresponding energies in an attempt to shed light on what appears to be a puzzle. Such measurements should be feasible in the foreseeable future.

2. Antiproton and antineutron annihilation on the proton

The OBELIX collaboration measured total annihilation cross sections for antiprotons on the proton [4, 5, 6] and for antineutrons on the proton [7]. From the results shown in fig.1 it is seen that whereas the $\bar{p}$ and $\bar{n}$ cross sections tend to be very close to each other above 200 MeV/c very large differences appear below $\approx$ 80 MeV/c. The $\bar{n}$ cross sections show moderate increase of cross sections as the energy goes down, most likely due to the expected $1/v$ dependence of the s-wave cross section. However the increase of the cross sections for the $\bar{p}$ is much stronger than the increase for $\bar{n}$. This is the result of the so-called Coulomb focusing effect which has already been

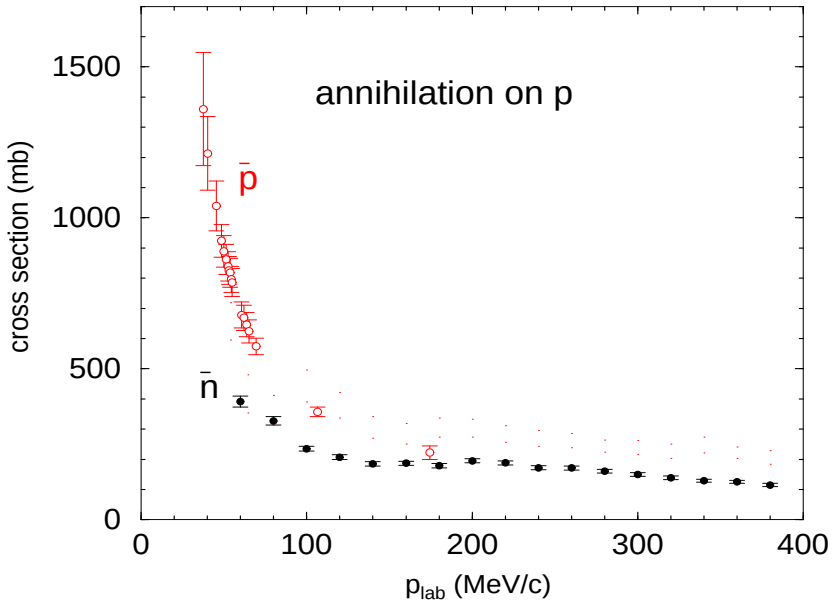

Figure 1: Total annihilation cross sections on the proton, from [4, 5, 6, 7]. Open circles for $\bar{p}$, filled circles for $\bar{n}$.

observed in annihilation cross sections of $\bar{p}$ on nuclei [8]. In situation of very strong absorption, typical of antiproton interactions, the 'black disk' cross section πR^2 is replaced by

$$\sigma_R = \pi R^2 (1 + \frac{2MZe^2}{\hbar^2 k_{\rm L} k R}) \tag{1}$$

with M the mass of the proton, k and $k_{\rm L}$ the cm and lab wave numbers, respectively and R the black disk radius. For very low energies (and momenta) the second term in the brackets becomes dominant. Note that the Z/R dependence increases very rapidly along the periodic table, considering that R changes with $A^{1/3}$, with A the mass number of the nucleus. It is therefore expected that annihilation cross sections for $\bar{p}$ on nuclei will increase as energy is lowered much faster than do the corresponding cross sections for antineutrons.

3. Antiproton-nucleus interaction

With energies close to threshold, we begin with antiprotonic atoms, where the experimental results of the PS209 collaboration at CERN [9] provided high-quality data for several sequences of isotopes along the periodic table. Detailed analyses of these results have been published in a series of papers, dedicated each to a particular subset of the data such as neighboring nuclei or isotopes of the same element. In the present context we discuss only *global* fits of optical potentials to the entire set of 90 data points relating to strong interaction level shifts and widths in $\bar{p}$ atoms [10].

In line with other types of exotic atoms [2], the interaction of antiprotons with nuclei at threshold is described in terms of an optical potential, which in the simplest $t\rho$ form is given by

$$2\mu V_{\rm opt}(r) = -4\pi(1+\frac{\mu}{M}\frac{A-1}{A})[b_0(\rho_n+\rho_p)+b_1(\rho_n-\rho_p)] \quad , \qquad (2)$$

where μ is the reduced mass of the $\bar{p}$, ρ_n and ρ_p are the neutron and proton density distributions normalized to the number of neutrons N and number of protons Z, respectively, $A = N + Z$, and M is the mass of the nucleon. The complex parameters b_0 and b_1 are determined by fits to the data; in the impulse approximation they are the isoscalar and isovector hadron-nucleon scattering lengths, respectively. The factor $(1+\frac{\mu}{M}\frac{A-1}{A})$ transforms these from the two-body CM system to the $\bar{p}$-nucleus CM system [11, 12]. A Coulomb potential due to the finite size charge of the nucleus was also included in the interaction together with vacuum polarization corrections. The optical potential is used in a Klein-Gordon (KG) equation to calculate strong interaction observables to be compared with experiment. Note that the KG equation yields to a very good approximation the j-averaged results from the Dirac equation. This is adequate as the PS209 experimental results do not distinguish between the different j values.

For the nuclear densities the ρ_p may be obtained from the generally known charge distribution by unfolding the 'finite size' of the proton but various simplifications are required in modelling ρ_n. The difference between the rms radii of the neutron and proton distributions turned out to be a significant factor in determining strong-interaction level shifts and widths in $\bar{p}$ atoms [10, 13, 14] and these differences are parameterized by a linear dependence on the relative neutron excess, namely

$$r_n - r_p = \gamma\frac{N-Z}{A} + \delta \ , \qquad (3)$$

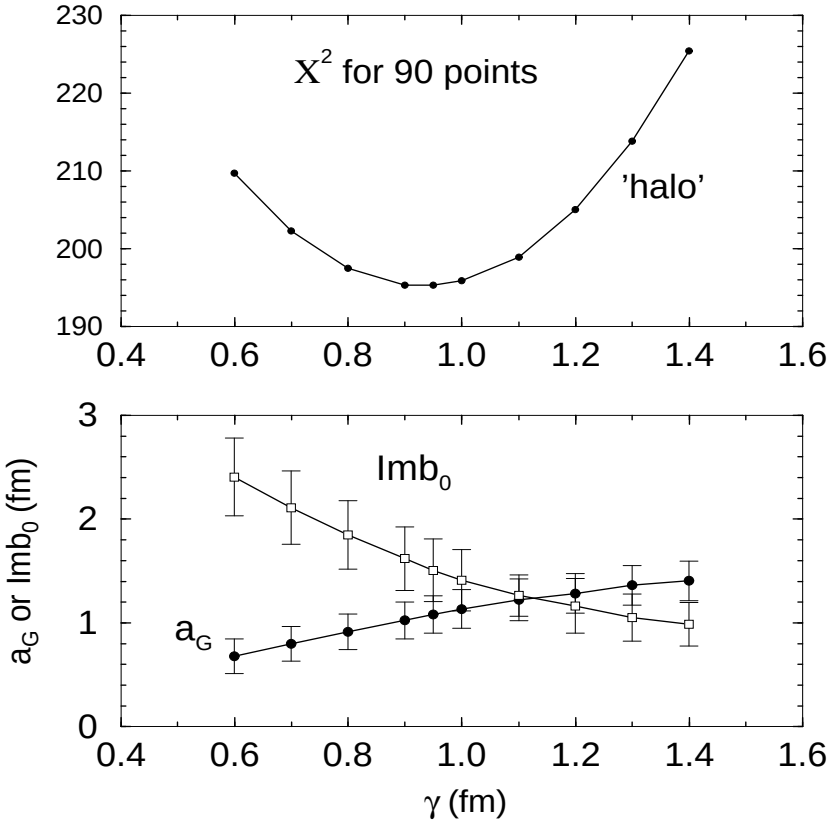

Figure 2: Summary of global fits to $\bar{p}$ atoms as function of the neutron density parameter γ of Eq.(3). Top: χ^2 values for 90 data points, bottom: resulting parameters Im b_0 and a_G, see text.

with γ close to 1.0 fm and δ close to zero. Two-parameter Fermi distributions are used for ρ_p and ρ_n with the 'halo' shape chosen for the latter where the larger r_n in nuclei with neutron excess is due to larger diffuseness parameter [13, 10]. In addition it was shown [10, 15] that introducing a finite-range folding into the otherwise zero-range potential Eq.(2) leads to significantly improved agreement between calculation and experiment in global fits to the data.

Results of global fits to 90 data points for $\bar{p}$ atoms with a finite range interaction are shown in fig.2 using $\delta = -0.035$ fm. Three parameters, Reb_0, Imb_0 and a_G were adjusted for each value of the parameter γ of Eq.(3), where

a_G is the range parameter of a Gaussian representing a finite range interaction with rms radius of $(3/2)^{1/2}a_G$. Almost identical results are obtained if a Yukawa interaction replaces the Gaussian, provided the two have the same rms radius. Earlier work [10] showed that at the minimum of χ^2 the isovector parameter b_1 is consistent with zero. The real part of the potential plays a relatively minor role compared to the imaginary part because of the very strong annihilation of antiprotons on nuclei. The best fit implies χ^2 per degree of freedom χ^2/d.f.= 2.2 for 29 different nuclei between ^{16}O and ^{208}Pb [10].

Next we examine the $\bar{p}$-nucleus potential at low energies above threshold which we wish to use for comparisons with $\bar{n}$-nucleus interactions. Measurements of elastic scattering of antiprotons by ^{12}C, ^{40}Ca and ^{208}Pb were made in the mid 80s and analyzed using standard low-energy optical model methods, see Janouin et al. [16] and references therein. Here we show that a potential very similar to the one derived from fits to $\bar{p}$ atoms is capable of describing the elastic scattering of antiprotons by nuclei near 300 MeV/c (48 MeV energy).

Above threshold the optical potential was used to calculate the complex phase shifts δ_l for several partial waves from which the observables were calculated. For example, the total reaction cross section which for $\bar{p}$ and $\bar{n}$ represents, to a very good approximation, the annihilation cross section, is given by

$$\sigma_R = (\pi/k^2)\Sigma(2l+1)T_l \tag{4}$$

where k is the c.m. wave number and the transmission T_l is given by

$$T_l = 1 - \exp(-4 \text{ Im } \delta_l). \tag{5}$$

In a first phase we considered the elastic scattering of 48 MeV antiprotons by ^{12}C and ^{40}Ca where the nuclear densities for ^{12}C were of the modified harmonic oscillator type [17]. For these targets of $N = Z$ nuclei there is no dependence on the parameter γ of Eq.(3) and the comparisons between calculation and experiment involve only the three parameters b_0 and a_G. Fits were made to the scattering data for the two targets put together leading to χ^2 of 127 for 68 data points. The resulting parameters are Re b_0 = (0.40 $\pm$ 0.04) fm, Im b_0 = (1.25 $\pm$ 0.05) fm and a_G = (1.34 $\pm$ 0.05) fm. Comparing with fig.2 we see agreement within errors with the Im b_0 and a_G values at the minimum of the χ^2 for $\bar{p}$ atoms. The same applies also to Re b_0, not shown in the figure. In a second phase we repeated the fit to

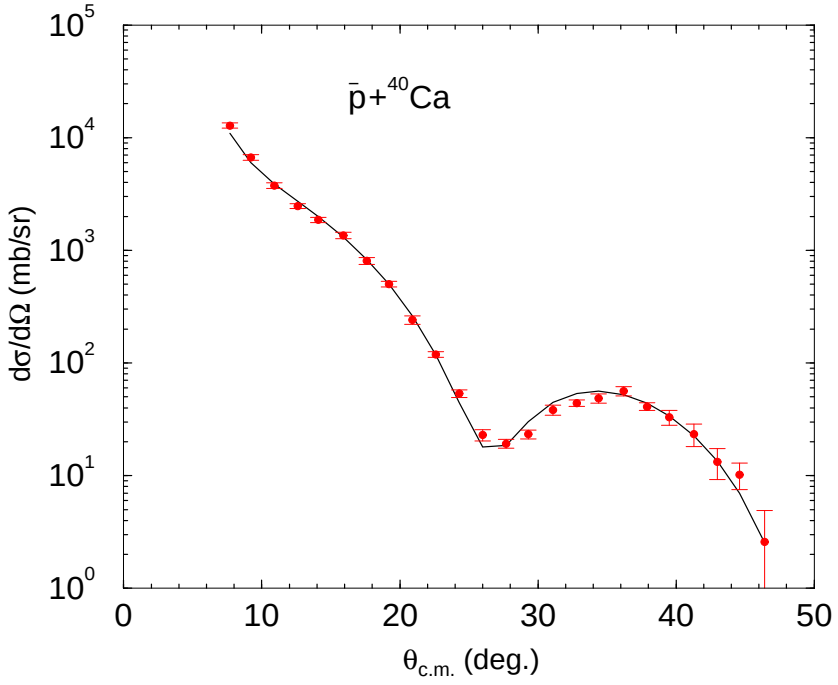

Figure 3: Comparing calculation with experiment for elastic scattering of 48 MeV antiprotons by ^{40}Ca. Data are from [16].

the scattering data for ^{12}C, ^{40}Ca and ^{208}Pb put together, a total of 88 data points. For ^{208}Pb a value of γ=0.9 fm was used following the best fit for $\bar{p}$ atoms. The quality of the fits and values of parameters remain the same as without ^{208}Pb, within errors. The χ^2/d.f. of 2.2 for the three targets, relating to five different experiments, is satisfactory. Note that only three parameters are required to achieve this result. Fig.3 shows as an example the fit to the experimental elastic scattering from ^{40}Ca. The overall picture hardly changes when the Gaussian folding is replaced by a Yukawa folding having the same rms radius. The present analysis can be extended up to 600 MeV/c [16] with very small changes in the final results.

Further tests of the potential model above threshold can be made with the small number of measured total annihilation cross sections for $\bar{p}$ on nuclei. These are compared to the calculated total reaction cross sections from the above optical potentials which could be somewhat larger than the annihilation cross sections above the threshold for charge exchange reactions. Table 1

Table 1: $\bar{p}$ annihilation cross sections on Ne. Experimental results from refs. [18] and [19].

p_{lab}(MeV/c)	57	192.8	306.2	607.9
σ_{exp}(mb)	2210±1105	956±47	771±28	623±21
σ_{calc}(mb)	2760	1040	865	676

Table 2: $\bar{p}$ annihilation cross sections at 100 MeV/c.Experimental results from ref.[20].

target	Ni	Sn	Pt
σ_{exp}(mb)	3300±1500	4200±900	8600±4100
σ_{calc}(mb)	3170	5560	8620

shows calculated total reaction cross sections with the experimental results of Bianconi et al. [18] and of Balestra et al. [19] for Ne. Similar comparisons are made in table 2 with the recent results of the ASACUSA collaboration at 100 MeV/c [20]. It is seen that the overall agreement between calculations based on the above optical model and experiment are satisfactory.

It is concluded that the interaction of antiprotons with medium-weight to heavy nuclei from sub-threshold $\bar{p}$ atoms up to 600 MeV/c is described well by an isoscalar optical potential that depends very little on energy.

4. Antineutron-nucleus interaction

Finally we turn to the annihilation cross sections of $\bar{n}$ on nuclei which was the main motivation for the present work. For lack of comparable set of experimental results for $\bar{p}$-nucleus interaction we base most of the comparisons (except for one point) on predictions made with the optical potential. Having demonstrated the ability of an optical potential to produce good fits to antiproton-nucleus observables across threshold without a need for an isovector term, it is natural to compare predictions made with the same optical potential with the experimental results for antineutron-nucleus interactions. Fig.4 shows (solid curves) comparison between calculations and experiment for four out of the six targets studies by Astrua et al. [1] where the calculations used the best-fit $\bar{p}$-nucleus potential of sec.3 also for antineutrons. It is seen that whereas above 250 MeV/c there is reasonable agreement between

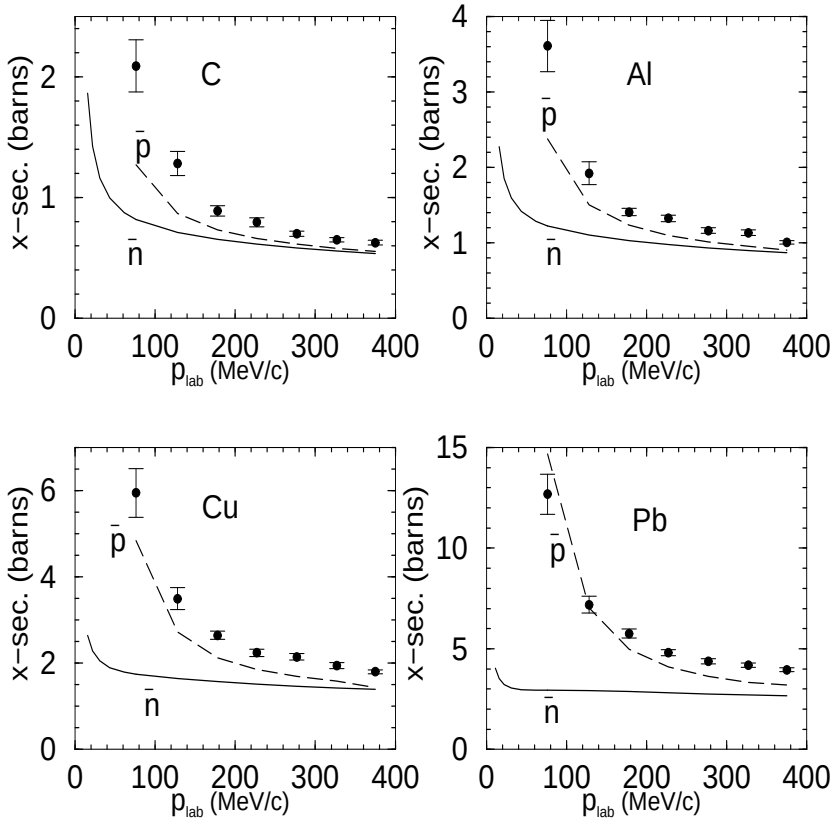

Figure 4: Comparing calculation with experiment for total annihilation cross sections on nuclei using the potential derived in sec.3. Solid curves for $\bar{n}$, dashed curves for $\bar{p}$. Experimental results for $\bar{n}$ are from [1].

calculation and experiment, the calculations underestimate experiment by up to a *factor* of 3-4 below 100 MeV/c. Moreover, calculations do not follow the trend of the experimental cross sections.

For lack of corresponding experimental results for antiprotons, fig.4 shows (dashed curves) also calculations for $\bar{p}$ annihilation cross sections on the same targets at the same energies using the optical potential derived in sec.3. Compared with the calculated $\bar{n}$ cross sections the Coulomb focusing effect is clearly seen, as expected. The start of the $1/v$ rise for $\bar{n}$ is also seen, shifting to lower and lower energies as the size of the nucleus increases.

Attempts to improve the agreement between calculations and experiment

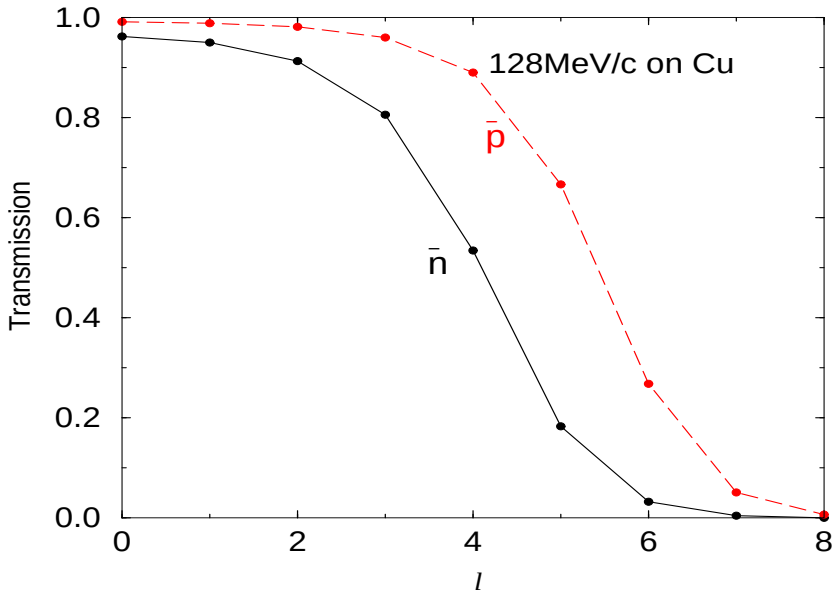

Figure 5: Transmission coefficients for 128 MeV/c antineutrons (solid curve) and antiprotons (dashed curve) on Cu as function of the angular momentum l calculated from the potential of sec.3.

for $\bar{n}$ by varying the potential parameters failed to reduce the huge discrepancies at the lower momenta unless the range parameter a_G was increased from 1.3 to 3.3 fm, implying a rms radius of 4.0 fm for the folding interaction. This value is significantly larger than e.g. the finite size of the proton or the pion Compton wavelength.

Insight into the working of the Coulomb focusing effect may be gained from fig.5 showing transmission coefficients for 128 MeV/c antineutrons (solid curve) and antiprotons (dashed curve) on Cu as function of the angular momentum l calculated from the potential of sec.3. The larger cross sections calculated with the Coulomb potentials included are due to the increase in the number of partial waves which contribute to the cross section with the $(2l+1)$ weight, see Eq.(5).

5. Discussion

Concluding that a simple global potential is capable of reproducing well all the experimental results on strong interaction effects in antiprotonic atoms

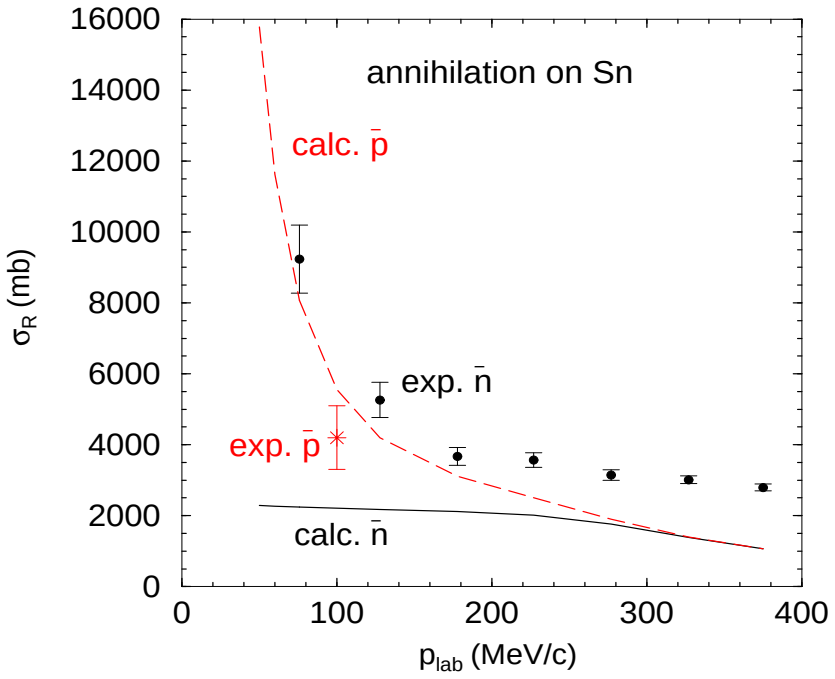

Figure 6: Comparing calculation with experiment for total annihilation cross sections on Sn using the potential derived in sec.3. Solid curve for $\bar{n}$, dashed curve for $\bar{p}$. Experimental results for $\bar{n}$ (filled circles) are from [1]. The single experimental point for $\bar{p}$ (star) is from [20], see also Table 2.

is not new [10]. We have shown here that the same potential produces also agreement with mesurements of elastic scattering of $\bar{p}$ by ^{12}C, ^{40}Ca and ^{208}Pb at 300 MeV/c and with the few measured annihilation cross sections on nuclei. This isoscalar potential has been used here to compare $\bar{n}$ and $\bar{p}$ cross sections on nuclei at very low energies.

In comparing total annihilation cross sections for antineutrons on nuclei with the corresponding values for antiprotons, one may be guided by fig.1 which shows that at very low energies the $\bar{p}p$ cross sections exceed significantly the $\bar{n}p$ ones. If the mechanism is the Coulomb focusing then the effect is expected to become stronger as the atomic number of the nucleus increases. This is indeed observed with calculated cross sections based on an optical potential which fits all the available experimental results for $\bar{p}$-nucleus interactions across threshold. Unfortunately comparable experimen-

tal results for $\bar{p}$ and $\bar{n}$ exist only for the proton as a target and we had to use optical potentials for comparisons with the $\bar{n}$-nucleus experimental results. However, there is a single experimental result which could be useful in this respect, namely, a preliminary result of the ASACUSA collaboration for the total annihilation cross section of $\bar{p}$ on Sn at 100 MeV/c [20]. Table 2 shows it to agree with the predictions of the optical potential and in fig.6 we see it in relation to the $\bar{n}$ cross sections on the same target. The figure suggests that the $\bar{n}$ cross sections are larger than the corresponding $\bar{p}$ cross sections, contrary to the evidence from fig. 1.

A possible conclusion that the $\bar{n}$-nucleus total annihilation cross sections at very low energies are equal to or larger than the corresponding $\bar{p}$ cross sections will be at variance with expectations based on smooth optical potentials and on experimental results for the proton as a target. A theoretical approach that may explain all the observations has not been presented so far. However, an experimental approach to this 'puzzle' is possible in the foreseeable future by measuring total annihilation cross sections for antiprotons on the six nuclear targets of Astrua et al. [1] at the same energies.

Acknowledgements

I wish to thanks T. Bressani for useful discussions and for providing in numerical form the detailed results of ref. [7]. Discussions with A. Gal and A. Leviatan are gratefully acknowledged.

References

[1] M. Astrua et al., Nucl. Phys. A 697 (2002) 209.

[2] E. Friedman, A. Gal, Phys. Rep. 452 (2007) 89 and references therein.

[3] G.W. Greenlees, G.J. Pyle, Y.C. Tang, Phys. Rev. 171 (1968) 1115.

[4] A. Bertin et al., Phys. Lett. B 369 (1996) 77.

[5] A. Zenoni et al., Phys. Lett. B 461 (1999) 405.

[6] A. Benedettini et al., Nucl. Phys. B (Proc. Suppl.) 56A (1997) 58.

[7] A. Bertin et al., Phys. Lett. B 410 (1997) 344.

[8] C.J. Batty, E. Friedman, A. Gal, Nucl.Phys. A 689 (2001) 721.

[9] A. Trzcińska et al., Nucl. Phys. A 692 (2001) 176c.

[10] E. Friedman, A. Gal, J. Mareš, Nucl. Phys. A 761. (2005) 283.

[11] C.J. Batty, E. Friedman, A. Gal, Phys. Rep. 287 (1997) 385.

[12] M.L. Goldberger, K.M. Watson, Collision Theory, John Wiley, New York, 1964.

[13] A. Trzcińska et al., Phys. Rev. Lett. 87 (2001) 082501.

[14] J. Jastrzębski et al., Int. J. Mod. Phys. E 13 (2004) 343.

[15] E. Friedman, Hyperfine Interact 193 (2009) 33.

[16] S. Janouin et al., Nucl. Phys. A 451 (1986) 541.

[17] H. de Vries et al., At Data Nucl. Data Tables 36 (1987) 495.

[18] A. Bianconi et al., Phys. Lett. B 481 (2000) 194.

[19] F. Balestra et al., Nucl. Phys. A 452 (1986) 573.

[20] A. Bianconi et al., Phys. Lett. B 704 (2011) 461.